PHYSICAL REVIEW B **86**, 054204 (2012)

Disorder-induced cavities, resonances, and lasing in randomly layered media

Yury Bliokh
Department of Physics, Technion-Israel Institute of Technology, Haifa 32000, Israel and Advanced Science Institute, RIKEN, Wako-shi, Saitama 351-0198, Japan

Elena I. Chaikina, Noemí Lizárraga, and Eugenio R. Méndez
División de Física Aplicada, Centro de Investigación Científica y de Educación Superior de Ensenada, Carretera Ensenada-Tijuana No. 3918, Ensenada, Baja California, 22860 Mexico

Valentin Freilikher
Department of Physics, Jack and Pearl Resnick Institute, Bar-Ilan University, Israel and Advanced Science Institute, RIKEN, Wako-shi, Saitama 351-0198, Japan

Franco Nori
Advanced Science Institute, RIKEN, Wako-shi, Saitama 351-0198, Japan and Department of Physics, University of Michigan, Ann Arbor, Michigan 48109-1040, USA

(Received 5 June 2012; revised manuscript received 12 August 2012; published 23 August 2012)

We study, theoretically and experimentally, disorder-induced resonances in randomly layered samples and develop an algorithm for the detection and characterization of the effective cavities that give rise to these resonances. This algorithm enables us to find the eigenfrequencies and to pinpoint the locations of the resonant cavities that appear in individual realizations of random samples for arbitrary distributions of the widths and refractive indices of the layers. Each cavity is formed in a region whose size is a few localization lengths. Its eigenfrequency is independent of the location inside the sample and does not change if the total length of the sample is increased by, for example, adding more scatterers on the sides. We show that the total number of cavities N_{cav} and resonances N_{res} per unit frequency interval is uniquely determined by the size of the disordered system and is independent of the strength of the disorder. In an active amplifying medium, part of the cavities may host lasing modes whose number is less than N_{res}. The ensemble of lasing cavities behaves as distributed feedback lasers, provided that the gain in the medium exceeds the lasing threshold, which is specific for each cavity. We present the results of experiments carried out with single-mode optical fibers with gain and randomly located resonant Bragg reflectors (periodic gratings). When the fiber was illuminated by a pumping laser with an intensity high enough to overcome the lasing threshold, the resonances revealed themselves by peaks in the emission spectrum. Our experimental results are in good agreement with the theory presented here.

DOI: 10.1103/PhysRevB.86.054204 PACS number(s): 42.55.Ah, 42.25.Fx, 71.55.Jv

I. INTRODUCTION

Anderson localization of waves in one-dimensional (1D) random media is associated with an exponential decrease in the wave amplitude inside the disordered locally transparent sample, which results in an exponentially small typical transmittance $T_{\mathrm{typ}} \propto \exp(-L/l_{\mathrm{loc}}) \ll 1$ (where L is the length of the sample and l_{loc} is the localization length). Another manifestation of Anderson localization is the existence of resonant frequencies where the transmission increases drastically, sometimes up to unity. These frequencies correspond to the quasilocalized eigenstates (modes or disorder-induced resonances) characterized by a high concentration of energy in randomly located points inside the system.

Even though 1D localization has been intensively studied during the past few decades[1] (see also Refs. 2 and 3 and references therein), most of the analytical results were obtained for mean quantities, i.e., for values averaged over ensembles of random realizations. These results are physically meaningful for the self-averaging Lyapunov exponent (inverse localization length), which becomes nonrandom in the macroscopic limit.[2] For non-self-averaging quantities (field amplitude and phase, intensity, transmission, and refection coefficients, etc.), a random system of any size is always mesoscopic, and therefore, mean values have little to do with measurements on individual samples. This is most pronounced when it comes to the disorder-induced resonances whose parameters are extremely volatile and strongly fluctuate from realization to realization.[4,5] In particular, ensemble averaging wipes out all information about the frequencies and locations of individual localized states within a particular sample, even though these data are essential for applications based on harnessing micro- and nanocavities with high-Q factors.

A. Disorder-induced cavities and resonances

Nowadays, photonic crystals are believed to be the most suitable platforms for the creation and integration of optical resonators into optical networks. To create an effective resonant cavity that supports localized high-Q modes in a photonic crystal (PC), it is necessary to break periodicity, i.e., to introduce a defect in a regular system. As fluctuations of the dielectric and geometrical parameters are inevitably present in any manufactured periodic sample, it could create a serious obstacle in the efficient practical use of PCs. Therefore, considerable efforts of researchers and manufacturers go into the

control of fluctuations. Alternatively, if rather than combating imperfections of periodicity, one fabricated highly disordered samples, they could be equally well harnessed, for example, for creating tunable resonant elements. This is because 1D random configurations have a unique band structure that, for some applications, has obvious advantages over those of a PC.[6] Contrary to periodic systems, resonant cavities inherently exist in any (long enough) disordered sample or can be easily created by introducing a nonrandom element (for example, homogeneous segment) into an otherwise random configuration. The effective wave parameters of these cavities are very sensitive to the fine structure of each sample and can be easily tuned either by slightly varying the refractive index in a small area inside the sample or, for example, by changing the ratio between the coupling strength and the absorption. This makes shifting the resonant frequency (and thereby locking and unlocking the flow of radiation), coupling modes, and creating quasiextended states, etc., possible[7,8]

It has been shown[9] that each localized state at a frequency $\omega = \omega_{\rm res}$ could be associated with an effective high-Q-factor resonance cavity composed of an almost transparent (for this frequency) segment bounded by essentially nontransparent regions (effective barriers). Wave tunneling through such a system can be treated as a particular case of the general problem of the transmission through an open resonator.[10] The distinguishing feature of a disorder-induced cavity is that it has no regular walls (the medium is locally transparent in each point), and high reflectivity of the confining barriers is due to the Anderson localization. Moreover, different segments of the sample are transparent for different frequencies, i.e., each localized mode is associated with its own resonator.

B. Random lasers

If the medium inside such a cavity is amplifying, the combination of the optical gain and the interference of multiply scattered radiation creates a coherent field and gives rise to multifrequency lasing with a sharply peaked lasing spectrum. Random lasers (RLs) are the subject of increasing scientific interest due to their unusual properties and promising potential applications.[11–17] Unlike conventional lasers where any disorder is detrimental, in a random version, scattering plays a positive role in increasing the path length and the dwell time of light in the active medium. So far, most studies, both experimental and theoretical, have concentrated on three-dimensional (3D) disordered systems and chaotic cavities. One of the grave drawbacks of 3D random lasers is their inefficient pumping, which is hampered by the scattering of the pumping radiation in the random medium. A one-dimensional RL, which is free from this disadvantage, can be realized either as a random stack of amplifying layers[18] or as a set of Bragg gratings (BGs) randomly distributed along a doped optical fiber.[19] In the last case, the wavelength of the pumping laser is shifted from the Bragg resonance of the gratings, and the fiber is excited homogeneously along the whole length of the sample. Both these methods noticeably reduce the lasing threshold as compared to the 3D random lasing systems. Because the frequencies of the modes and the locations of the effective cavities randomly vary from sample to sample, in most cases, they are described statistically.[20–24] However, usually, we deal with a specific random sample, and it is important to know how many modes and at which frequencies they can be excited in a given frequency range where these modes are localized inside this sample, etc.[11]

Another field of research, in which this information was crucial, recently arose after it had been realized that Anderson resonances could be used to observe cavity quantum electrodynamics effects by embedding a single quantized emitter (quantum dot) in a disordered PC waveguide.[25,26] In those experiments, the efficiency of the interaction between radiation and disorder-induced cavities depends strongly on the location of the source inside the random sample. Indeed, all QED effects are well pronounced when the emitter with a given frequency is placed inside the effective cavity, which is resonant at this frequency, and could be completely suppressed otherwise.

In this paper, we develop an algorithm that enables detecting all cavities and finding their locations and eigenfrequencies for any *individual* sample with given geometry and optical parameters. It is shown that, in the case of uncorrelated disorder, the number of disorder-induced resonances per unit frequency interval is independent of the strength of the fluctuations and is uniquely determined by the size of the random sample. The results have been checked experimentally using RLs based on a single-mode fiber with randomly distributed resonant Bragg gratings developed in Ref. 19.

II. DISORDER-INDUCED CAVITIES AND RESONANCES

In Refs. 6, 7, 9, and 10, it has been shown that, for a quantitative description of the wave propagation through a disordered sample, it is advantageous to consider it as a random chain of effective regular resonators with given Q factors and coupling coefficients. The typical size of each resonator is on the order of the localization length $l_{\rm loc}$, and their centers are randomly distributed along the sample. For manufacturing RLs and for the ability to tailor their properties, it is important to know the location of the resonant cavity for each eigenfrequency.[11] To this end, a criterion is necessary, which enables determining whether a given area of a disordered sample is either a resonant cavity or a strongly reflecting (typical) random segment.

To derive such a criterion for randomly layered media, we consider a disordered sample consisting of N homogeneous layers with thicknesses d_j and dispersionless refractive indices n_j ($j = 1,2,\ldots,N$) that are statistically independent and are uniformly distributed in the intervals $(d_0 - \delta d, d_0 + \delta d)$ and $(n_0 - \delta n, n_0 + \delta n)$, respectively. (The effects of correlation between the thicknesses of the adjacent blocks have been considered in Refs. 27–29.) In a system with uncorrelated layers, the interface between the jth and the $(j+1)$-th layers is located at a random point z_j and can be characterized by complex transmission t_j and reflection r_j coefficients, which are also randomly distributed in the corresponding intervals. The numeration is chosen from left to right so that $z_j < z_{j+1}$. It is assumed, thereafter, that the optical contrast between layers is small. Therefore, all Fresnel reflection coefficients r_j are also small,

$$|r_j| \ll 1, \tag{1}$$

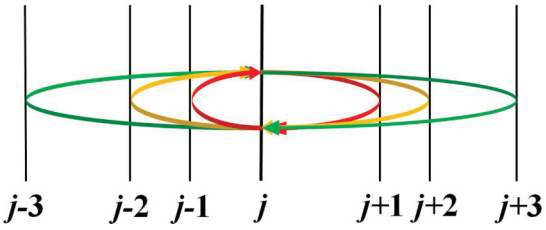

FIG. 1. (Color online) Schematic of closed trajectories in a randomly layered sample.

and, consequently, $1 - |t_j|^2 \ll 1$. For the sake of simplicity, these coefficients will be assumed to be real. The generalization for complex valued r_j and t_j is straightforward.

In what follows, it is convenient to turn to the *optical lengths*, i.e., to replace the thicknesses d_j and the coordinates z_j by

$$\tilde{d}_j = n_j d_j, \quad \tilde{z}_j = \sum_{i<j} n_i z_i, \tag{2}$$

where n_j is the refraction index of the jth layer. Note that, in these notations, the wave number has the same value $\tilde{k} = k = \omega/c$ in all layers.

To distinguish between an effective resonator and a Bragg reflector, a proper physical quantity representative of distinctive properties of these objects has to be found. To do this, let us consider a wave that propagates rightward from a point $\tilde{z} = \tilde{z}_j + 0$ [right side of the interface between the $(j-1)$-th and the jth layers] where its amplitude is $A_{j0}^{(+)}$ (thereafter, superscripts $(+)$ and $(-)$ denote the amplitudes of the waves propagating to the right or to the left, respectively). After traveling through the jth layer, the wave is partially reflected back from the interface between the jth and the $(j+1)$-th slabs. The transmitted part extends through the $(j+1)$-th layer and is partially reflected from the next interface, etc. (see Fig. 1).

If the scattering at the interfaces between layers is weak, Eq. (1), the amplitude $\tilde{A}_j^{(-)}$ of the total field reflected from the N_s layers and returned back to the point $\tilde{z} = \tilde{z}_j + 0$ can be calculated in the single-scattering approximation and is equal to

$$\tilde{A}_j^{(-)} = r_j^{(+)}(k)\, A_{j0}^{(+)}, \tag{3}$$

where

$$r_j^{(+)}(k) = \sum_{m=1}^{N_s} r_{j+m} \exp[2ik(\tilde{z}_{j+m} - \tilde{z}_j)], \tag{4}$$

and $k = \omega/c$ is the wave number. The amplitude $\tilde{A}_j^{(+)} = r_j^{(-)}(k)\, A_{j0}^{(-)}$ is introduced in the same way, with the *left* reflection coefficient $r_j^{(-)}(k)$,

$$r_j^{(-)}(k) = -\sum_{m=0}^{N_s} r_{j-m} \exp[2ik(\tilde{z}_j - \tilde{z}_{j-m})]. \tag{5}$$

In Eq. (5), it is taken into account that the reflection coefficients r_l and r_r for waves that are incident on the same interface from the left or from the right have opposite signs: $r_l = -r_r$. The field of all waves that made a *closed path* and returned back after consequent reflections from the N_s layers located on the right and the N_s layers located on the left from the jth layer has an amplitude $A_{j1}^{(+)}$. In the general case, $A_{j1}^{(+)}$ is not equal to the initial amplitude $A_{j0}^{(+)}$, and the difference is

$$\delta A_j^{(+)} = A_{j0}^{(+)} - A_{j1}^{(+)} \equiv A_{j0}^{(+)}[1 - \Delta_j(k)], \tag{6}$$

where

$$\Delta_j(k) = r_j^{(+)}(k)\, r_j^{(-)}(k). \tag{7}$$

The function $\Delta_j(k)$ is an important characteristic, which uniquely determines the resonant properties of any one-dimensional wave system. In particular, the eigen-numbers can be found as poles of the Green's function, i.e., as the roots of the equation,[30,31]

$$\Delta_j(k) - 1 \equiv r_j^{(+)}(k)\, r_j^{(-)}(k) - 1 = 0. \tag{8}$$

In the case of a closed resonator,

$$\Delta(k) = \exp(2i\pi n), \qquad n = 1,2,3, \ldots,$$

i.e., $\arg\,\Delta(k) = 2\pi n$, and $\mathrm{Re}\,\Delta(k) = 1$. For an open resonant cavity, the roots k_{res} of Eq. (8) are complex $k_{\mathrm{res}} = k_R + ik_I$. If the Q factor of a resonator is large enough, then $k_R \gg k_I$, and

$$\mathrm{Re}\,\Delta(k_R) = 1 - k_R \ell/Q \; > 0, \tag{9}$$

$$\mathrm{Im}\,\Delta(k_R) \simeq 0, \tag{10}$$

where ℓ is the resonator length.

Note that Eq. (10) also is fulfilled when $\arg\,\Delta(k) = \pi n$, which is the Bragg reflection condition. In this case, in contrast to a resonant cavity, $\mathrm{sgn}\{r^{(+)}(k)\} = -\mathrm{sgn}\{r^{(-)}(k)\}$, and the real part of $\Delta(k)$ is negative $\mathrm{Re}\,\Delta(k) < 0$.

These properties of the quantity $\Delta(k)$ are quite general and can be used to characterize randomly layered systems, in particular, to detect effective resonant cavities inside them. Indeed, when for a segment of $2N_s$ layers centered at a point $\tilde{z}_j$ inside a long ($N \gg N_s$) disordered sample the imaginary part of $\Delta(k)$ is zero at some $k = \omega/c$, this area is either a resonant (at the frequency ω) cavity or a localization-induced resonant Bragg reflector. What it is, indeed, is determined by the sign of the real part of Δ: In a resonator, $\mathrm{Re}\,\Delta > 0$, whereas, for a Bragg grating, $\mathrm{Re}\,\Delta < 0$.

The last condition is easy to understand if we notice that $r_j^{(+)}(k)$ is the $(-2k)$-Fourier harmonics of the function,

$$F_j^{(+)}(z) = \sum_{m=1}^{N_s} r_{j+m}\delta[\tilde{z} - (\tilde{z}_{j+m} - \tilde{z}_j)], \tag{11}$$

and $r_j^{(-)}(k)$ is the $(+2k)$-Fourier harmonics of the function,

$$F_j^{(-)}(z) = \sum_{m=0}^{N_s} (-r_{j-m})\delta[\tilde{z} - (\tilde{z}_{j-m} - \tilde{z}_j)]. \tag{12}$$

This means that $r_j^{(+)}(k)$ and $r_j^{(-)}(k)$ are Bragg reflection coefficients from N_s slabs located to the right and to the left of the jth layer, respectively.

Since our prime interest here is disorder-induced resonators for which $|r_j^{(\pm)}| \sim 1$ and because, in the localized regime, the reflection coefficient from a typical region is close to unity when its length is on the order (and larger) of the localization

length, for further calculations, we have to choose $N_s = l_{\rm loc}/d_0 \equiv N_{\rm loc}$. It is important to stress that each resonator is formed in an area of the size of a few localization lengths and is practically unaffected by the outer (to this area) parts of the sample. This means that the eigenfrequency of an effective cavity is independent of it location inside a sample and does not change if the total length of the sample is increased, for example, by adding more scatterers at its edges. When the thicknesses of the layers are uncorrelated and the mean thickness $\overline{\widetilde{d}_j} = \widetilde{d}_0$ is large compared to the wavelength $k\widetilde{d}_0 \gg 2\pi$, the localization length is determined by the mean value of the local reflection coefficients r_j.[32] To prove this statement, note that the functions $r_j^{(\pm)}(k)$, Eqs. (4) and (5), are sums of $N_{\rm loc}$ uncorrelated random complex numbers and, therefore, can be described in terms of a random walk on the plane ($\mathrm{Re}\, r$,$\mathrm{Im}\, r$) with the single step equal to $|r_j|$. Then, the mean absolute value $\overline{|r_j^{(\pm)}(k)|}$ is the mean distance from the origin after $N_{\rm loc}$ steps: $\overline{|r_j^{(\pm)}(k)|} = \overline{|r_j|}\sqrt{N_{\rm loc}} \sim 1$, and therefore,

$$N_{\rm loc} \simeq (\overline{|r_j|})^{-2}. \tag{13}$$

The characteristic scale of the variation in $r_j^{(\pm)}(k)$ along the sample measured in a number of layers is on the order of $N_{\rm loc} \gg 1$. Thus, the coefficients $r_j^{(\pm)}(k)$, and hence, the quantities $\Delta_j(k)$ are smooth random functions of j, i.e., of the distance along the sample. As the length N of a sample is large enough $N \gg N_{\rm loc}$, the number of regions where $\mathrm{Re}\,\Delta_j(k) > 0$ is approximately equal to the number of regions where $\mathrm{Re}\,\Delta_j(k) < 0$. The characteristic size of these areas is the localization length. Therefore, the expected *number of cavities* $N_{\rm cav}$, resonant at a given wave number k is as follows:

$$N_{\rm cav} \simeq \frac{\widetilde{L}}{2l_{\rm loc}}. \tag{14}$$

In order to estimate the *number of resonances* $N_{\rm res}$ in a given interval Δk of the wave numbers (in a given frequency interval $\Delta\omega = c\,\Delta k$), it is necessary to estimate the cavity "width," $\delta k_{\rm res}$ in the k domain. To do this, we note that the variation δk in the wave number leads to a variation $\delta\varphi_j$ in $\varphi_j \equiv \arg\,\Delta_j(k)$,

$$\delta\varphi_j = \delta k\frac{d\varphi_j}{dk} = \mathrm{Im}\left\{\frac{1}{\Delta_j(k)}\frac{d\Delta_j(k)}{dk}\right\} = \delta\kappa\left[\mathrm{Im}\frac{1}{r_j^{(+)}(k)}\frac{dr_j^{(+)}(k)}{dk} + \mathrm{Im}\frac{1}{r_j^{(-)}(k)}\frac{dr_j^{(-)}(k)}{dk}\right]. \tag{15}$$

The resonant wave number k_r is defined by the condition (10), therefore, the second resonance appears in a small vicinity of the same layer j when the variation in $\arg\,\Delta_j(k)$ approaches 2π: $\delta\varphi_j \simeq 2\pi$. It is easy to see that the largest contribution to $\delta\varphi_j$ comes from the layers that are the most distant from the jth layer,

$$\mathrm{Im}\frac{d}{dk}[\ln\, r_j^{(\pm)}(k)] \sim \left|\widetilde{z}_j - \widetilde{z}_{j\pm N_{\rm loc}}\right| \sim N_{\rm loc}\widetilde{d}_0 = l_{\rm loc}. \tag{16}$$

Thus, $\delta\varphi_j(k) \sim 2\,\delta k\, l_{\rm loc}$ and the characteristic interval $\delta k_{\rm res}$ between resonant wave numbers localized around an arbitrary point $\widetilde{z}_j$ can be estimated as

$$\delta k_{\rm res} \simeq \frac{\pi}{l_{\rm loc}}. \tag{17}$$

In Ref. 9, this result has been obtained for modes located around the center of the sample.

Equations (14) and (17) allow estimating the number of resonances $N_{\rm res}$ in the given frequency interval $\Delta\omega = c\,\Delta k$ in the sample of the length N,

$$N_{\rm res} = N_{\rm cav}\frac{\Delta k}{\delta k_{\rm res}} \simeq N\,\Delta k\,\widetilde{d}_0/2\pi. \tag{18}$$

The number of cavities $N_{\rm cav}$ and the spacing between the resonances $\delta k_{\rm res}$ are inversely proportional[9] to $l_{\rm loc}$, i.e., it increases when the strength of the scattering increases. Therefore, from Eq. (18), it follows that $N_{\rm res}$ does not depend on the localization length. In other words, the number of resonances (and, therefore, the number of peaks in the transmission spectrum and the number of regions with enhanced intensity) in a given frequency interval is proportional to the size of the random system and is independent of the strength of disorder.

An important point is that Eq. (18) gives the *total* number of disorder-induced resonances existing along the whole length of a random system in a given range Δk. When random lasing is concerned, each sample is an active medium, and a new parameter—the specific gain rate g—should be involved. In evaluating the number of *lasing* modes, this parameter has to be compared with the lasing threshold $g_c^{(j)}$ of each cavity, which is different for different ones. In Ref. 9, as has been shown and mentioned in the Introduction above, each disorder-induced resonator occupying an area $z_{j-N_s} \leqslant z \leqslant z_{j+N_s}$ is built of strongly reflecting (as a result of Anderson localization) effective barriers that confine an almost transparent (for the given resonant wave number k) region. Reflection coefficients of the left and right (from the center) parts of this structure are large, which means that the normalized amplitudes $f_{\mp 2k}^{(\pm)}$ of the $\pm 2k$ harmonics of the distributions $F_j^{(\pm)}$ [Eqs. (11) and (12)] of the scatterers in these parts of the jth cavity are large $|f_{\mp 2k}^{(\pm)}| \sim 1$. However, the value f_{2k} of the amplitude of the $2k$ harmonics of the distribution $F_j(z) = F_j^{(+)}(z) - F_j^{(-)}(z)$ of the scatterers along the *whole* cavity can be small or even equal to zero. Indeed, since

$$f_{2k} = f_{-2k}^{(+)*} + f_{2k}^{(-)} = r^{(+)*} - r^{(-)},$$

$$|f_{2k}|^2 = |r^{(+)}|^2 + |r^{(-)}|^2 - 2\,\mathrm{Re}\,\Delta(k),$$

and

$$|r^{(+)}| \sim |r^{(-)}| \sim 1,$$

the value of $|f_{2k}|$ is small when $\mathrm{Re}\,\Delta(k)$ is close to unity. For given values of $|r^{(+)}|$ and $|r^{(-)}|$, the smaller the amplitude $|f_{2k}|$, the greater $\mathrm{Re}\,\Delta(k)$. In the extreme case, the amplitude $|f_{2k}|^2$ turns to zero, i.e., the $2k$ harmonics is completely suppressed. This happens when the amplitudes $f_{\mp 2k}^{(\pm)}$ have equal absolute values but opposite signs, i.e., are shifted in phase by π. Thus, the (positive) value of $\mathrm{Re}\,\Delta(k)$ can be treated as a measure of the amplitude of the $2k$ harmonics of the cavity and of the phase shift between the $2k$ harmonics of its left and right parts.

In a real random sample, the $2k$ harmonics of the spatial distributions $F_j^{(\pm)}(z)$ of the scatterers are not equal to zero in any effective cavity and for any k (any frequency ω), including the resonant ones. These harmonics provide distributed feedback (DFB) as it occurs, for instance, in a conventional (not random) semiconductor DFB laser (see, e.g., Ref. 33). As in a conventional DFB laser with regular Bragg grating (regular periodic spatial distribution of the scatterers), in a disorder-induced cavity, a lasing mode is excited when the gain rate g of the medium exceeds the value $g_c^{(j)}$ of the threshold of the cavity. The difference between these two cases is that the whole periodic grating is characterized by a single value of g_c, whereas, different parts of a random configuration have their own different thresholds $g_c^{(j)}$, whose values are minimal into the cavities. In just the same way as the phase shift between two identical halves of the regular grating causes a decrease in the threshold in conventional DFB lasers,[33] the phase difference between complex amplitudes $f_{2k}^{(-)}$ and $f_{-2k}^{(+)}$ reduces the lasing threshold of the $2k$-resonant random cavity. From the considerations presented in the previous paragraph, it follows that the information about $g_c^{(j)}$ is also contained in the quantities Δ_j: The greater $\mathrm{Re}\,\Delta_j(k)$ is for a given cavity, the smaller is its threshold $g_c^{(j)}$. Thus, only those cavities whose thresholds $g_c^{(j)}$ are less than the medium gain g [i.e., the values $\mathrm{Re}\,\Delta_j(k)$ exceed the critical value Δ_c], contribute to the formation of the lasing spectrum. Therefore, the number of lasing modes (number of lines in the lasing spectrum) is definitely smaller than the total number of cavities N_{res}.

To conclude this section, we note that the approach presented above could be used in studying various wave systems, for example, terahertz tunable vortex photonic crystals. Indeed, many calculations on this problem have already been performed,[34] including the role of disorder, but this is beyond the scope of this paper.

III. NUMERICAL SIMULATIONS

To verify the results of the previous section, we have calculated the function $\Delta_j(k)$ numerically for different random samples and have found the distribution of the areas with $\mathrm{Re}\,\Delta_j(k) > 0$ and $\mathrm{Re}\,\Delta_j(k) < 0$ along each sample for different wave numbers. These distributions have been mapped on the coordinate-wave-number plane in Fig. 2.

Then, the eigenvalues k_{res} have been determined from Eq. (8), and spatial distributions of the intensity created inside the samples by the incident waves with the corresponding resonant frequencies ($\omega_{\mathrm{res}} = ck_{\mathrm{res}}$) have been found and have been compared with the map. To facilitate this comparison, we take into account that the intensity pumped by the incident wave into a cavity depends on its location inside the sample: It decreases exponentially as the distance of the cavity from the input end increases.[9,35] As an example, the intensity distributions along the same sample, illuminated by the same wave, either from the left $I_l(j)$ (blue curve) or from the right $I_l(j)$ (red curve) ends are shown in Fig. 3(a).

In both curves shown in Fig. 3, the intensity in the closest to the input cavity is far above the intensity inside the more distant

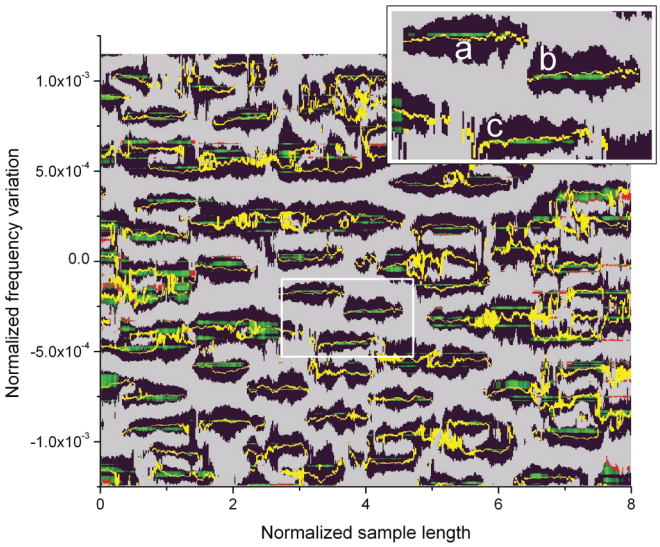

FIG. 2. (Color online) Mapping of $\Delta_j(k)$ and the normalized resonant intensities $I_s(j,k)$ on the coordinate-frequency plane. The units on the x axis are normalized to the localization length. In the black areas $\mathrm{Re}\,\Delta_j(k) > 0$, the gray color corresponds to $\mathrm{Re}\,\Delta_j(k) > 0$. Approximately half of the full length of any line $k = \omega/c =$ constant is occupied by black areas where the cavities are located. The yellow (light gray) color marks the regions where $|\arg\,\Delta_j(k) - 2\pi| < 0.05$. The regions with a strong concentration of the wave field where $I_s(j,k) > 1/2$ are marked in green (dark gray). As can be seen, practically all of them are located in the cavities (black areas) as predicted here. Inset: enlarged view of the selected area with three (a–c) resonances.

one. Therefore, we have introduced the normalized quantity,

$$I_s(j) = \frac{\left[\frac{I_l(j)}{\max\{I_l(j)\}} + \frac{I_r(j)}{\max\{I_r(j)\}}\right]}{\max\left\{\left[\frac{I_l(j)}{\max\{I_l(j)\}} + \frac{I_r(j)}{\max\{I_r(j)\}}\right]\right\}}, \tag{19}$$

which is symmetric with respect to the direction of incidence and reveals all resonators equally well, independent of their positions Fig. 3(b).

In Fig. 2, regions where $\mathrm{Re}\,\Delta_j(k) > 0$ and $\mathrm{Re}\,\Delta_j(k) < 0$ are marked by black and gray, respectively, the normalized intensity $I_s(j,k)$ is shown by the green color. The yellow color marks the regions where $|\arg\,\Delta_j(k) - 2\pi| < 0.05$. One can see that any horizontal cross section $k =$ constant contains approximately the same number of black and blue regions, and practically all resonances are located in black areas associated with cavities as predicted.

Examples of the spatial distributions of $\mathrm{Re}\,\Delta_j$(blue curves) for three resonant frequencies marked by a–c in Fig. 2 are presented in Fig. 4 along with the corresponding distributions of the intensity (red curves). Shown in Fig. 5, cross-correlation functions $C(l) = \sum_j \mathrm{Re}\,\Delta_j I_{j-l}$ of those two types of curves reveal a strong correlation between the normalized intensity and $\mathrm{Re}\,\Delta$. One can see that the cavities are well detected by the $\mathrm{Re}\,\Delta > 0$ criterion.

Figure 6 demonstrates that, in accordance with Eq. (18), the number of resonances in a given frequency interval is independent of the strength of disorder (of the values of the local reflection coefficients r_j) and of the variance in the

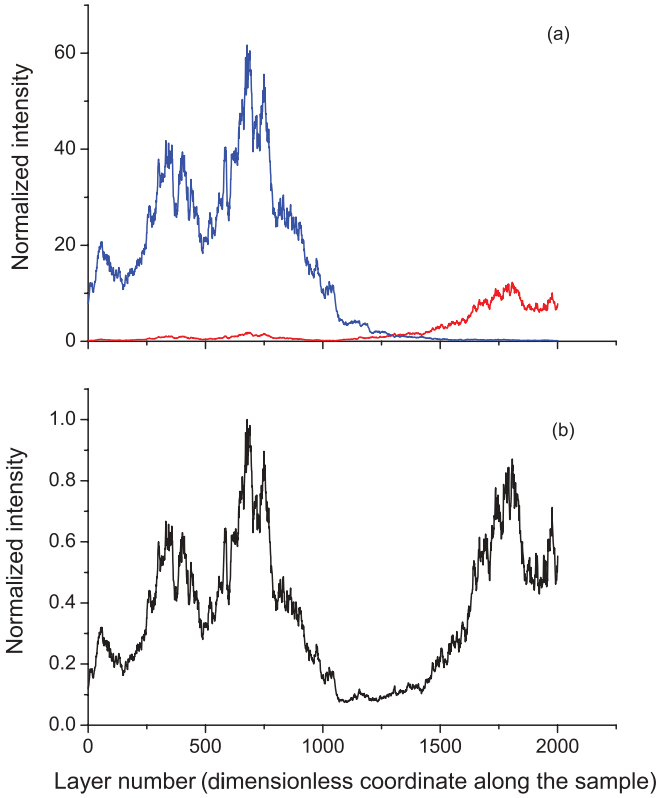

FIG. 3. (Color online) (a) Spatial distributions of the intensity generated by a wave incident from the left (thin blue curves) and right (thick red curves) sides of the sample; (b) intensity normalized in accordance with Eq. (19). The incident wave generates a resonance (peak in the intensity) only in the cavity closest to the edge it is coming from. The distribution of the normalized intensity is independent of the direction of incidence and clearly reveals all cavities resonant at a given frequency.

fluctuations of the thicknesses d_j and is completely determined by the size of the sample.

This rather counterintuitive result is also supported by the numerical simulations presented in Fig. 7 where the locations of the resonant cavities in the coordinate-frequency plane are shown (marked in black) for two samples. The samples are geometrically identical, i.e., have the same spatial distribution of the scatterers, and differ only in the amplitudes of their reflection coefficients so that the localization length in the upper picture is twice larger than in the lower panel. When comparing both images in Fig. 7, it is easy to see that, in passing from one picture to another, the sizes of the black areas in the x direction increase, whereas, the distances between them along the y axis decrease in the same proportion so that, in keeping with Eq. (18), N_{res} remains the same, meaning that there is no dependence of the number of resonances on the localization length.

IV. EXPERIMENTS WITH ACTIVE RANDOM SAMPLES: NUMBER OF LASING MODES

The experimental detection of disorder-induced cavities and resonances is a challenging task in optics. Although the intensity distribution cannot be measured directly, the resonances, in principle, can be revealed by transmission experiments at different frequencies. However, although resonant transmission in lossless systems is essentially higher than at typical frequencies, it is much stronger affected by absorption, which is proportional to the exponentially large intensity inside the resonators. In microwave experiments[6,7] where the absorption length was much larger than the total length of the system (single-mode waveguide), the transmission was below the noise level even at centrally located resonances. This fact was of little concern in that case because the microwave probe could be inserted in different points inside the waveguide. In fiber-optic systems, however, this is not possible. With long optical fibers to make the transmission measurable, it might be necessary to compensate for the absorption by, for example, introducing amplification. When the amplification is

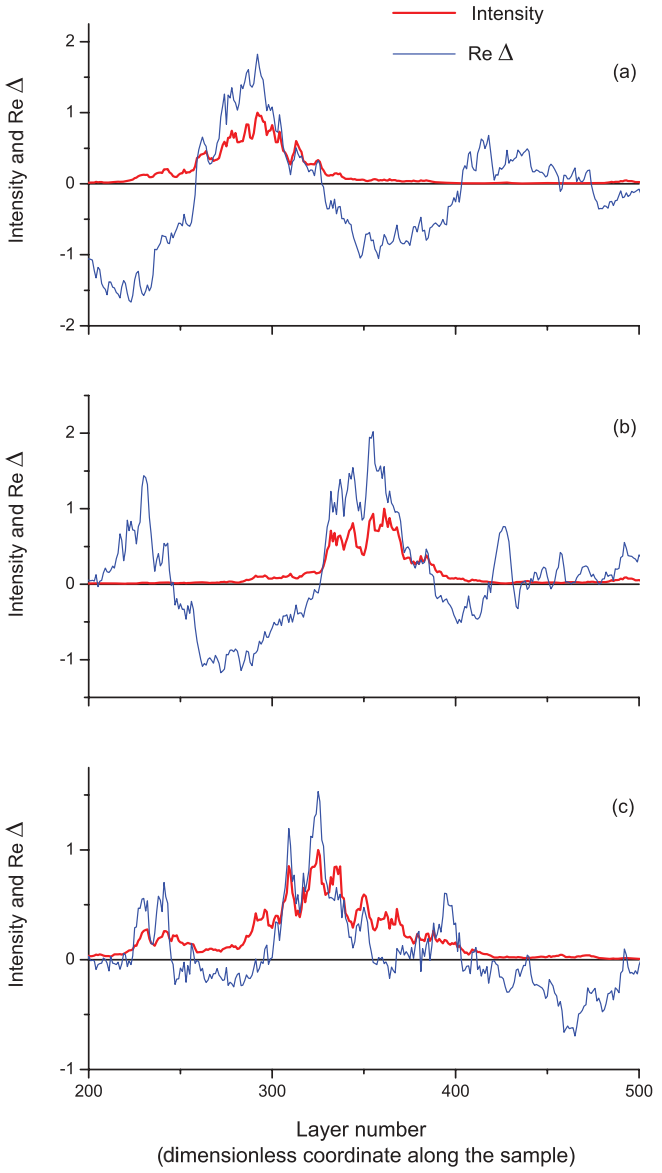

FIG. 4. (Color online) Spatial distributions of Re Δ_j (thin blue curves) and of the normalized intensity (thick red curves) for three resonant wave numbers marked by a–c in the inset in Fig. 2. One can see that each resonance is localized in the area where Re Δ_j is positive and takes a maximal value.

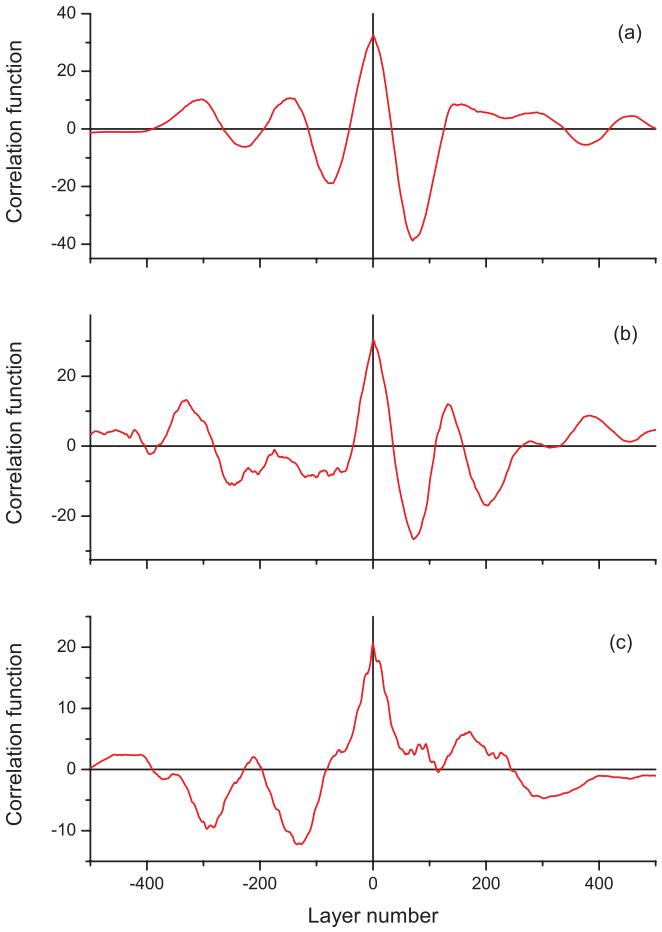

FIG. 5. (Color online) Cross-correlation functions $C(l) = \sum_j \mathrm{Re}\,\Delta_j I_{j-l}$ of the normalized intensity and Re Δ for three resonant wave numbers marked by a–c in the inset in Fig. 2. The curves reveal a strong correlation between the normalized intensity and Re Δ.

sufficiently large, all resonances manifest themselves as sharp lines in the transmission spectrum.

Experimental studies of resonances in disordered optical fibers with active elements is also of interest for a better understanding of the physics of RLs because, in amplifying media, all resonant modes are potential candidates for lasing. The ability to monitor and to tailor their parameters, especially the total number, eigenfrequencies, and locations is critical to fulfill this potential.

Random one-dimensional cavities can be created in optical fibers by the introduction of randomly positioned reflectors in the form of Bragg gratings.[36] To create such structures, we have used commercial Er/Ge co-doped fibers (INO, Quebec City, Quebec, Canada) that are single modes at 1535 nm. Erbium is the active element, and germanium doping provides a kind of photosensitivity that can be used to locally change the refractive index. The Bragg gratings were fabricated by exposing the fiber to UV light (244 nm) from a frequency-doubled argon-ion laser through a periodic mask whose spatial period is 1059.8 nm. Each one of the fabricated gratings had a length of approximately 5 mm. The random distances between the gratings were statistically independent and uniformly distributed in the interval $d_0 \pm 0.8$ mm where

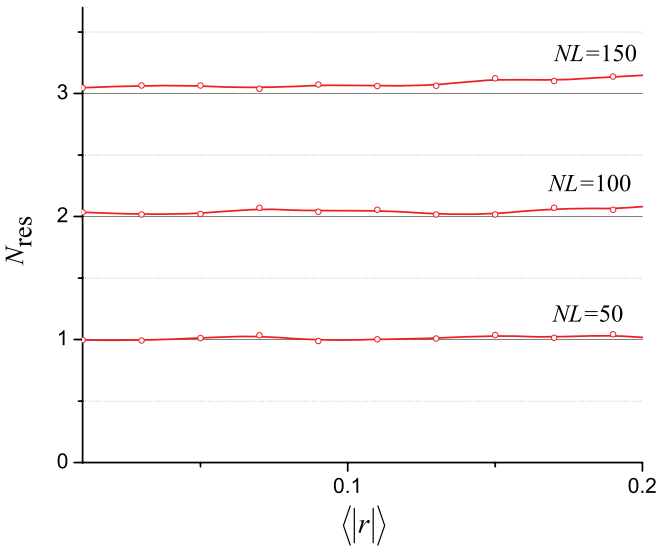

FIG. 6. (Color online) Number of resonances N_{res} as a function of the averaged local reflection coefficient (strength of disorder) $\langle |r| \rangle$. It is easy to see that, as predicted by the theory, the number of resonances in a given frequency interval grows linearly with the size of the sample and is independent of the strength of the disorder. Parameters of the numerical simulations: $k\tilde{d}_0 = 10.0$, $\Delta k\,\tilde{d}_0 = 0.1$. Each point is obtained by averaging over 10^3 random samples.

the mean distance between gratings d_0 was approximately 5 mm.

The fabricated Bragg gratings have a narrow reflection spectrum (its full width at half maximum is about 0.17 nm) centered at 1535.3 nm with a maximum reflectivity of about 0.07–0.08. Under these conditions, the estimated localization length is found to be about five to six gratings. We notice that variations in the mask alignment, recording exposure, and fiber tension during the writing process caused small

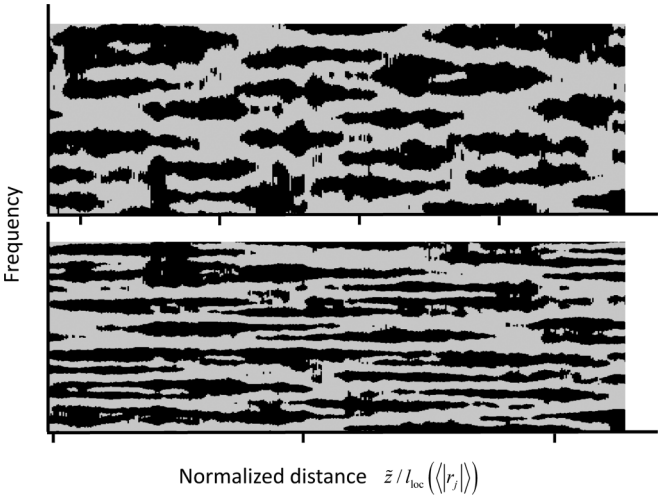

FIG. 7. Distribution of the resonant cavities in the coordinate-frequency plane for two geometrically identical samples with different strengths of the scattering and, thus, with different localization lengths. Top: $\langle |r_j| \rangle = 0.2$; bottom: $\langle |r_j| \rangle = 0.15$. The distances between the black tick marks under each picture are equal to the corresponding localization lengths.

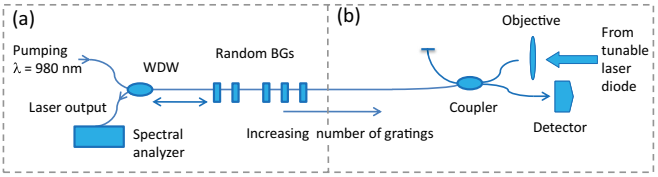

FIG. 8. (Color online) Schematic of the experimental setup. In (a), we illustrate the configuration of the laser. The wavelength-division multiplexing (WDM) device permits the separation of the pump (980 nm) and lasing radiation (1550 nm). In (b), we show the arrangement used to measure the reflection spectrum of the grating array during the fabrication process.

variations in the central wavelength of the gratings and on the sharpness of their reflection spectra. As a result, the half-width of the reflection spectrum of an array of 31 gratings is about 0.27 nm.

The optical arrangement employed to fabricate the gratings and to measure the reflection spectra of the arrays is illustrated in Fig. 8. Laser action was obtained by end pumping the system with 980-nm radiation from a semiconductor laser. A WDM was used to separate the pumping wavelength from the radiation emitted by the laser (see Fig. 8). Measurements of the gratings transmission/reflection coefficients with a spectral

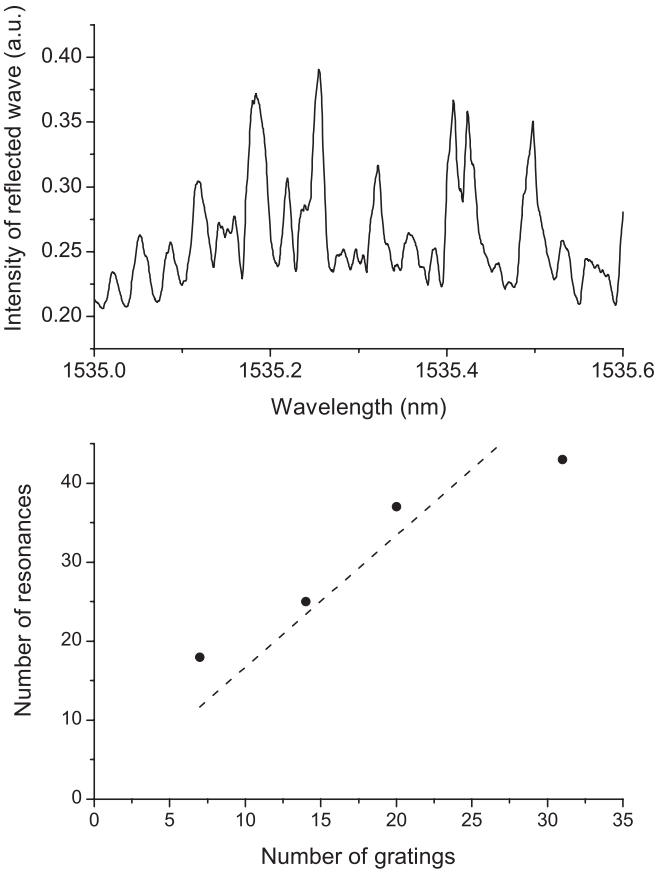

FIG. 9. Top: experimental reflection spectrum from an array of 14 gratings. Bottom: experimental (black points) and theoretical (dotted line) dependence of the number of resonances $N_{\rm res}$ on the number of gratings N_g. The theoretical dependence is calculated using Eq. (18) and the parameters of the experiments.

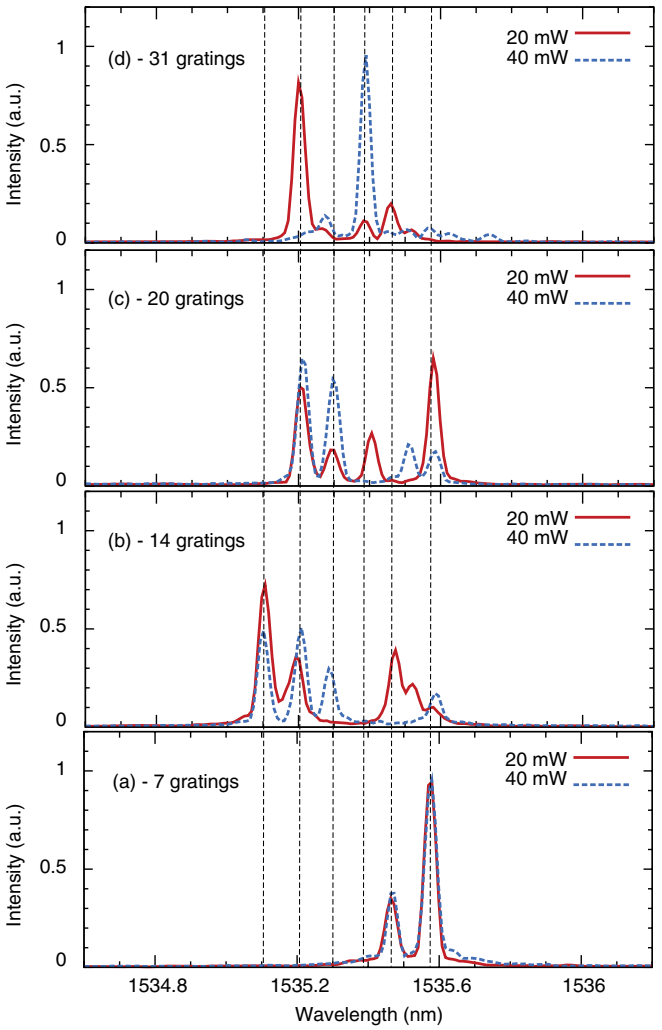

FIG. 10. (Color online) Emission spectra of the samples with 7, 14, 20, and 31 gratings for 20-mW (green) and 40-mW pumping powers. Both values are well above the lasing threshold. The vertical lines mark the spectral positions of the emission lines.

resolution of 0.001 nm were carried out in the spectral range of 1520–1580 nm, using a tunable semiconductor laser (New Focus Velocity 6300) with a coherence length of a few meters. As illustrated in the figure, new gratings were fabricated in the sequence, beginning from the pumping end of the fiber.

To explore the dependence of the total number of resonances $N_{\rm res}$ on the size of the system, we measured the frequency spectrum of the reflection coefficient on samples with different numbers of reflectors and made use of the fact that each resonance manifested itself as a sharp drop in the reflectivity. Black points in Fig. 9 represent the total number of the resonances detected in the arrays of different numbers of gratings N_g (different lengths of the samples $L = N_g d_0$, $d_0 = 5$ mm) in the wavelength range (1534.8–1535.6 nm). The theoretical prediction Eq. (18), $N_{\rm res} = 1.67 N_g$ (dotted line), is in excellent agreement with the experimental data.

In Fig. 10, we present the results of the measurements of the emission spectra of the RL fiber containing 7, 14, 20, and 31 randomly distributed Bragg gratings for two values of the pumping power: 20 mW, denoted by the continuous-line

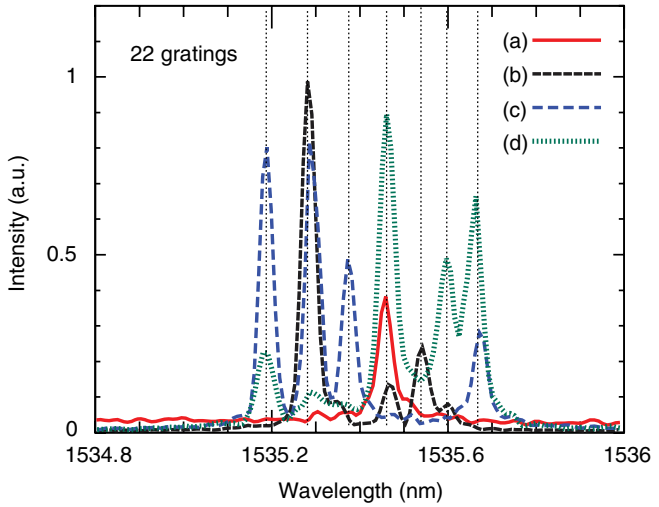

FIG. 11. (Color online) Emission spectra of the sample with 22 gratings generated by the fixed pumping power (40 mW) at different moments in time.

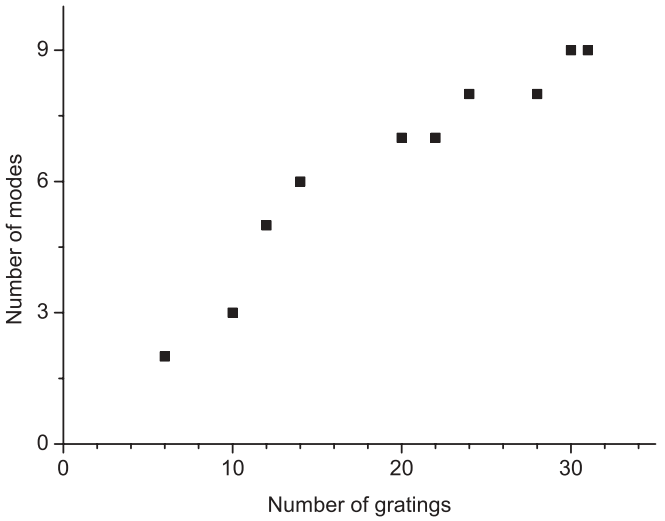

FIG. 12. Number of resonances measured in the wavelength range of $\lambda \pm \Delta\lambda = 1.5 \times 10^{-4} \pm 0.85 \times 10^{-8}$ cm (black points) as a function of the number of Bragg reflectors. Since the total length of the sample is proportional to the number of gratings, the figure actually presents the dependence on the size of the random system.

curves and 40 mW, denoted by the dashed-line curves. With these pump levels, the systems were above threshold in all cases. For the measurements, we used a spectrum analyzer with a resolution of 0.01 nm.

From Fig. 10, one can see that, in the considered frequency range, the emission spectrum contains several peaks that reveal the presence of resonant modes. As the number of gratings grows, so does the number of resonances: There are two peaks for the RL with 7 gratings and seven peaks for the sample with 20 gratings. For the RL with seven gratings, the two peaks maintain their positions and relative intensities as the pump power increases. For systems with a higher number of gratings, the competition between modes produces temporal fluctuations in the relative strengths of the emission lines; these fluctuations also depend on the pump power. Although the relative intensity in the peaks can change with the pump power, their spectral positions (indicated by the vertical lines in the figure) remain fixed.

Another interesting feature that can be observed in Fig. 10 is that, once an emission line appears in a system with a low number of gratings, it is likely to reappear in a system with a higher number of gratings. One can see, for example, that the emission lines observed in the system with seven gratings are also present in the systems with more gratings.

The curves shown in Fig. 11 represent spectra of the radiation emitted by a random laser with 22 gratings, measured in 1-s intervals. Even at constant pumping power, the number of well-defined lasing modes and their emission intensity fluctuate in time. The emission frequencies, however, remain fixed; one can see that they always coincide with one of the vertical lines of the figure. The observed fluctuations in the intensity of the spectral lines could not be caused by relatively small ($\sim$5%) fluctuations in the intensity of the pumping laser and apparently were associated with nonlinear effects. Indeed, despite the relatively low power of the emission, the field inside the high-Q cavities can be strong enough (due to resonance) to generate a Kerr-type nonlinearity. These effects are of importance, for example, in distributed Bragg reflector fiber lasers that are longer than 20 cm.[37,38]

The black points in Fig. 12 denote the number of lasing modes measured in the wavelength range of $\lambda \pm \Delta\lambda = 1535.3 \pm 0.3$ nm in samples with different numbers of gratings N_g (and different lengths of the system; $L = N_g d_0$, $d_0 = 5$ mm). These numbers were obtained by adding all the emission lines present in the emission spectra over an extended period of time. The amount of the lasing modes growths linearly with the length of the system, although, in accordance with the theoretical reasoning above, it is always less than the total number of the effective resonant cavities in the sample (Fig. 9).

V. SUMMARY

To conclude, eigenmodes (resonances) of a randomly layered long ($L \gg l_{\mathrm{loc}}$) sample are localized in disorder-induced effective cavities of the size on the order of the localization length that are randomly distributed along the sample. An algorithm for finding this distribution in an individual configuration with arbitrary (random) parameters was developed based on the calculation of the function $\Delta_j(k)$ in Eq. (7). It was shown that a cavity of an effective size of a few localization lengths in which a mode with $k = k_{\mathrm{res}}$ can be localized exists around the jth layer when $\mathrm{Im}\,\Delta_j(k_{\mathrm{res}}) = 0$ and $\mathrm{Re}\,\Delta_j(k_{\mathrm{res}}) > 0$. In the case of uncorrelated disorder and weak scattering, the spacing between the eigenlevels and the number of cavities N_{res} in a given frequency interval does not depend on the strength of disorder and are uniquely determined by the size of the sample. The frequency of each resonance is independent of the coordinate of the effective cavity in which it is located. The number of lasing modes also depends on the ratio between the threshold values $g_c^{(j)}$ of the individual cavities and the gain g in the medium and is less than N_{res}. The theoretical predictions and numerical results are in reasonable agreement with the experimental data obtained by measuring the emission spectra of the random laser based on the single-mode fiber with randomly distributed Bragg gratings.

ACKNOWLEDGMENTS

F.N. is partially supported by the ARO, JSPS-RFBR Contract No. 12-02-92100, Grant-in-Aid for Scientific Research (S), MEXT Kakenhi on Quantum Cybernetics, and the JSPS via its FIRST program. V.F. is partially supported by the Israeli Science Foundation (Grant No. 894/10). We thank S. Ozdemir for his careful reading of the manuscript and useful comments.

[1] *50 Years of Anderson Localization*, edited by E. Abrahams (World Scientific, Singapore, 2010).
[2] I. M. Lifshits, S. A. Gredeskul, and L. A. Pastur, *Introduction to the Theory of Disordered Systems* (Wiley, New York, 1988).
[3] P. Cheng, *Introduction to Wave Scattering, Localization and Mesoscopic Phenomena* (Springer-Verlag, Heidelberg, 2006).
[4] M. Y. Azbel and P. Soven, Phys. Rev. B **27**, 831 (1983).
[5] M. Y. Azbel, Phys. Rev. B **28**, 4106 (1983).
[6] K. Y. Bliokh, Y. P. Bliokh, V. Freilikher, A. Z. Genack, B. Hu, and P. Sebbah, Phys. Rev. Lett. **97**, 243904 (2006).
[7] K. Y. Bliokh, Y. P. Bliokh, V. Freilikher, A. Z. Genack, and P. Sebbah, Phys. Rev. Lett. **101**, 133901 (2008).
[8] L. Labonté, C. Vanneste, and P. Sebbah, Opt. Lett. **37**, 1946 (2012).
[9] K. Y. Bliokh, Y. P. Bliokh, and V. D. Freilikher, J. Opt. Soc. Am. B **21**, 113 (2004).
[10] K. Y. Bliokh, Y. P. Bliokh, V. Freilikher, S. Savel'ev, and F. Nori, Rev. Mod. Phys **80**, 1201 (2008).
[11] N. Bachelard, J. Andreasen, S. Gigan, and P. Sebbah, Phys. Rev. Lett. **109**, 033903 (2012).
[12] H. Cao, Waves Random Complex Media **13**, R1 (2003).
[13] M. A. Noginov, *Solid-State Random Lasers* (Springer, Berlin, 2005).
[14] H. Cao, J. Phys. A **38**, 10497 (2005); D. S. Wiersma, Nat. Phys. **4**, 359 (2008).
[15] J. Andreasen, A. A. Asatryan, L. C. Botten, M. A. Byrne, H. Cao, L. Ge, L. Labonté, P. Sebbah, A. D. Stone, H. E. Türeci, and C. Vanneste, Adv. Opt. Photon. **3**, 88 (2011).
[16] B. N. S. Bhaktha, X. Noblin, and P. Sebbah, arXiv:1203.0091.
[17] J. Opt. **12**, 020201 (2010), special issue on light-induced material organization, edited by D. S. Wiersma and M. A. Noginov.
[18] V. Milner and A. Genack, Phys. Rev. Lett. **94**, 073901 (2005).
[19] N. Lizárraga, N. P. Puente, E. I. Chaikina, T. A. Leskova, and E. R. Méndez, Opt. Express **17**, 395 (2009).
[20] T. S. Misirpashaev and C. W. J. Beenakker, Phys. Rev. A **57**, 2041 (1998).
[21] O. Zaitsev, Phys. Rev. A **74**, 063803 (2006).
[22] O. Zaitsev, L. Deych, and V. Shuvayev, Phys. Rev. Lett. **102**, 043906 (2009).
[23] X. Jiang and C. M. Soukoulis, Phys. Rev. Lett. **85**, 70 (2000).
[24] X. Wu and H. Cao, Opt. Lett. **32**, 3089 (2007).
[25] L. Sapienza, H. Thyrrestrup, S. Stobbe, P. D. Garcia, S. Smolka, and P. Lodahl, Science **327**, 1352 (2010).
[26] H. Thyrrestrup, S. Smolka, L. Sapienza, and P. Lodahl, Phys. Rev. Lett. **108**, 113901 (2012).
[27] S. Tamura and F. Nori, Phys. Rev. B **41**, 7941 (1990).
[28] N. Nishiguchi, S. Tamura, and F. Nori, Phys. Rev. B **48**, 2515 (1993).
[29] N. Nishiguchi, S. Tamura, and F. Nori, Phys. Rev. B **48**, 14426 (1993).
[30] L. M. Brekhovskikh, *Waves in Layered Media* (Academic, New York, 1960).
[31] A. L. Burin, M. A. Ratner, H. Cao, and S. H. Chang, Phys. Rev. Lett. **88**, 093904 (2002).
[32] V. Freilikher, B. Lianskii, I. Yurkevich, A. Maradudin, and A. McGurn, Phys. Rev. E **51**, 6301 (1995).
[33] M. Okai, J. Appl. Phys. **75**, 1 (1994).
[34] S. Savel'ev, A. L. Rakhmanov, and F. Nori, Phys. Rev. Lett. **94**, 157004 (2005); Phys. Rev. B **74**, 184512 (2006); S. Savel'ev, V. A. Yampol'skii, A. L. Rakhmanov, and F. Nori, Rep. Prog. Phys. **73**, 026501 (2010).
[35] B. Payne, J. Andreasen, H. Cao, and A. Yamilov, Phys. Rev. B **82**, 104204 (2010).
[36] O. Shapira and B. Fischer, J. Opt. Soc. Am. B **22**, 2542 (2005).
[37] Y. H. Lian and H. G. Winful, Opt. Lett. **21**, 471 (1996).
[38] B. Liu, A. Yamilov, and H. Cao, Appl. Phys. Lett. **83**, 1092 (2003).